our previous study.[6,7] Briefly, we first examined all slides of IDCs that contained both tumor areas and nontumor areas to identify lymph vessel tumor emboli. Next, we selected the lymph vessel tumor emboli, for example, large lymph vessel tumor emboli far from the stroma-invasive tumor margin to examine for the presence and number of mitotic figures and apoptotic figures of lymph vessel tumor emboli in an IDC (Figures 1a and c). We classified all IDCs into the following four grades according to the number of mitotic and apoptotic figures in tumor cells in lymph vessels in one per high-power field: grade 0, no lymph vessel invasion; grade 1, absence of no mitotic and or apoptotic figures, or presence of any number of mitotic figures and absence of but no apoptotic figures, or absence of mitotic figure and presence of any number of apoptotic figures but no mitotic figures; grade 2, 1–4 mitotic figures and ≥ 1 apoptotic figures, or ≥ 1 mitotic figures and 1–6 apoptotic figures; and grade 3, >4 mitotic figures and >6 apoptotic figures. We selected the lymph vessel tumor emboli in which to count the mitotic figures and apoptotic figures and then recorded the numbers of mitotic figures and apoptotic figures among the tumor cells making up the lymph vessel tumor emboli of the IDC in the high-power field that contained the largest number of mitotic figures, and/or the largest number of apoptotic figures were recorded as the number of mitotic figures and apoptotic figure in the lymph vessel tumor emboli of the IDC. For the biopsy specimens, we examined the presence or absence of lymph vessel tumor

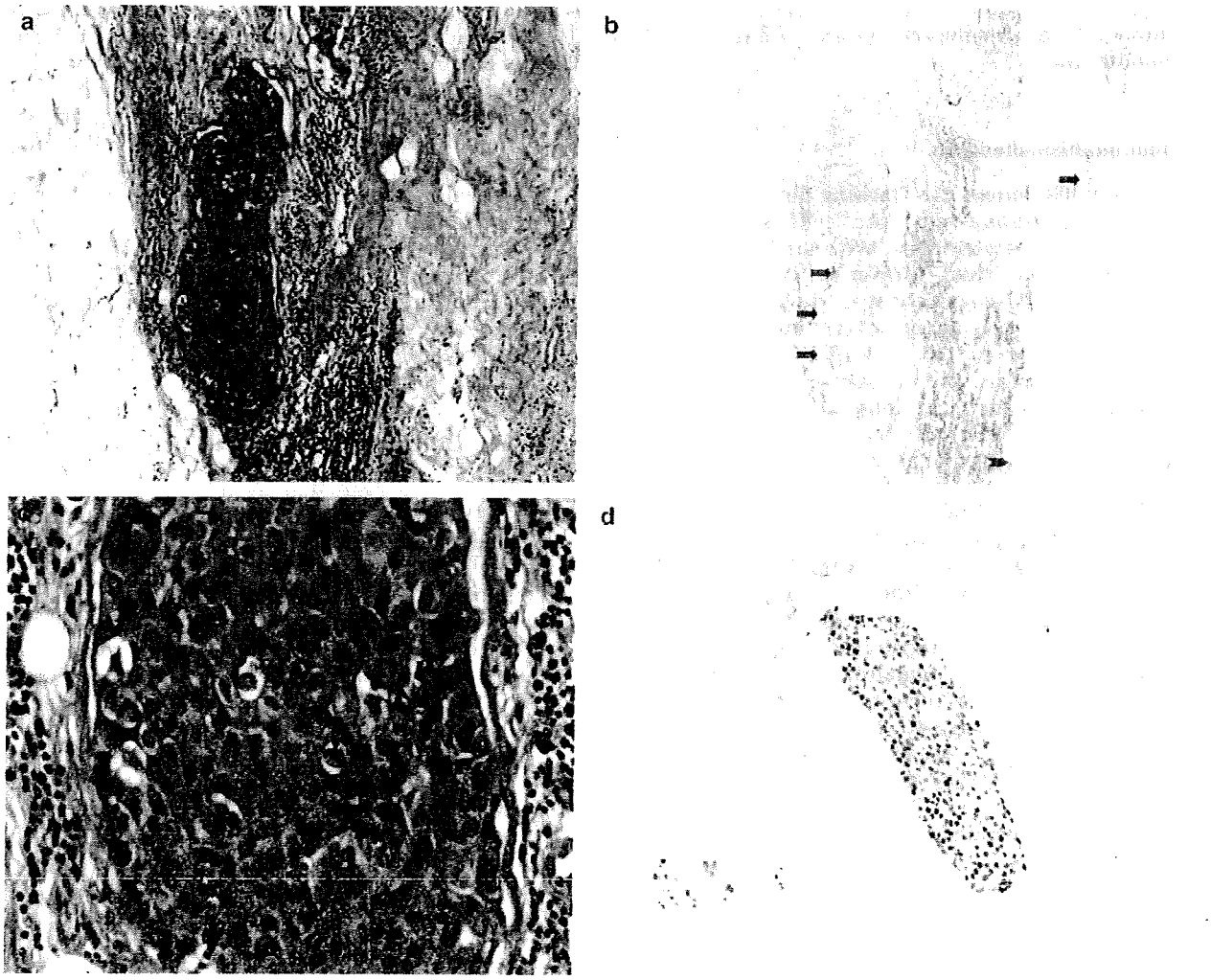

Figure 1 (**a**) Two lymph vessel tumor emboli are observed. (**b**) Vessel walls positive for D2-40 around two lymph vessel tumor emboli can be seen (arrows). One small lymph vessel is also positive for D2-40 (arrow), and one artery is negative for D2-40 (arrowhead). (**c**) Several apoptotic bodies and apoptotic tumor cells are observed (arrowheads), and there are five mitotic tumor cells (arrows) in tumor embolus in the lymph vessel. Apoptotic bodies are small, variously shaped pyknotic bodies that resemble sesame seeds, and apoptotic tumor cells were identified as tumor cells that contained eosinophilic or amphophilic cytoplasm and an irregularly shaped pyknotic nucleus. (**d**) Three lymph vessel tumor emboli with an Allred score of 8 for p53 can be seen. More than 90% of the tumor cells comprising of the lymph vessel tumor emboli show an intense nuclear staining for p53.

embolus or lymph vessel tumor emboli; when lymph vessel tumor embolus or lymph vessel tumor emboli were observed in the biopsy specimen, an assessment similar to that described above was performed. Some IDCs contained large lymph vessel tumor emboli, especially in IDCs containing a grade 2 or 3 lymph vessel tumor emboli, and it was difficult to determine whether they were true lymph vessel tumor emboli or a non-IDC component by hematoxylin and eosin staining alone. We therefore performed immunohistochemical staining with D2-40 antibody (monoclonal mouse antibody, Signet, Dedham, MA, USA, 1:200) to confirm that the lymph vessel tumor emboli identified by hematoxylin and eosin staining in some of the IDCs with grade 2 or 3 lymph vessel tumor emboli were true tumor emboli (Figure 1b). The D2-40 antibody was generated against an O-linked sialoglycoprotein having a molecular weight of 40 kDa and had been shown to be a selective marker of the lymphatic endothelium.[16,17]

Immunohistochemistry

Immunohistochemical staining for estrogen receptors, progesterone receptors, p53, HER2 products, and D2-40 was performed with an autoimmunostainer (Optimax Plus: BioGenex, San Ramon, CA, USA). The antigen retrieval device used for the Optimax Plus was an autoclave, and each specimen was immersed in citrate buffer and incubated at 121°C for 10 min. Immunoperoxidase staining was performed by using a labeled streptavidin biotin staining kit (BioGenex) according to the manufacturer's instructions. The antibodies used were an anti-estrogen receptor mouse monoclonal antibody (mAb), ER88 (BioGenex), an anti-progesterone receptor mAb, PR88 (BioGenex), and an anti-HER2 mAb, CB11 (BioGnex), and a p53 mAb, DO7 (Dako, Glostrup, Denmark). ER88, PR88, and CB11 were already diluted, and DO7 was applied at a 1:100 dilution. After immunostaining, the sections were counterstained with hematoxylin. Sections of IDCs positive for estrogen receptor, progesterone receptor, p53, HER2, and D2-40 were used each time as positive controls. As for a negative control, the primary antibody was replaced with normal mouse immunoglobulin.

Slides immunostained for estrogen receptor, progesterone receptor, and p53 in stroma-invasive tumor cells, and for p53 in tumor-stromal fibroblasts were scored by the Allred scoring system as previously described.[8,18–22] The highest intensity score, not the average intensity score, for nuclear expression of p53 was assigned for in tumor-stromal fibroblasts, and the highest p53 nuclear expression proportion score and intensity score were then to be evaluated in one high-power field ($\times 40$ objective and $\times 10$ ocular).[8] The Allred scores for estrogen receptor, progesterone receptor, and p53 expression in stroma-invasive tumor cells and tumor-stromal fibroblasts were classified into the following three categories: (1) Allred score for estrogen receptor in stroma-invasive tumor cells, 0 or 2, 3–6, and 7 or 8; (2) Allred score for progesterone receptor in stroma-invasive tumor cells, 0 or 2, 3–6, and 7 or 8; (3) Allred scores for p53 in stroma-invasive tumor cells, 0 or 2 or 3, 4–6, and 7 or 8; and (4) Allred scores for p53 in tumor-stromal fibroblasts, 0 or 2, 3, and 4–8. HER2 expression in stroma-invasive tumor cells was classified into the three categories: 0 or 1, 2, and 3.[23] We also assigned Allred scores for estrogen receptor, progesterone receptor, and p53 (Figure 1d), and HER2 category in lymph vessel tumor emboli by the similar manner as in stroma-invasive tumor cells in 26 of the 82 IDCs with lymph vessel invasion. We were unable to assign Allred scores for estrogen receptor, progesterone receptor, and p53, and HER2 category in the other IDCs with lymph vessel invasion, because immunohistochemistry for these was performed in tumor tissue sections that did not containing an lymph vessel tumor embolus.

One author (TH) assessed all the immunohistochemical parameters, and one of four other authors (NT, HT, TS, or YS) reviewed the immunohistochemical parameters to confirm the IDC immunohistochemical characteristics recorded by TH. Discordant results were reevaluated jointly to reach until a consensus was reached. The histological examination and immunohistochemical examination were performed without knowledge of the patient's outcome.

Patient Outcome and Statistical Analysis

Survival was evaluated by follow-up for a median period of 62 months (range: 38–105 months) until February 2009. As of the end of February 2009, 191 of the 281 patients were alive and well, 90 had developed tumor recurrence, and 53 had died of their disease. The measurements of tumor-recurrence-free survival, and overall survival started at the time of surgery. Tumor relapse was considered to have occurred whenever there was evidence of metastasis.

Multiple regression analysis was used to perform the statistical analyses for associations between lymph vessel tumor embolus grade and number of lymph node metastases, and the correlation analyses were performed by the correlation statistics of Cochran–Mantel–Haenszel statistics. We analyzed the outcome-predictive power for tumor recurrence and tumor-related death by the univariate and multivariate analyses using the Cox proportional hazard regression model. The factors analyzed were the mentioned eight factors, age (≤ 39, > 39 years), type of neoadjuvant therapy (endocrine therapy, chemotherapy and chemoendocrine therapy), adjuvant therapy (no, yes), and the factors that were significantly associated with outcome in the uni-

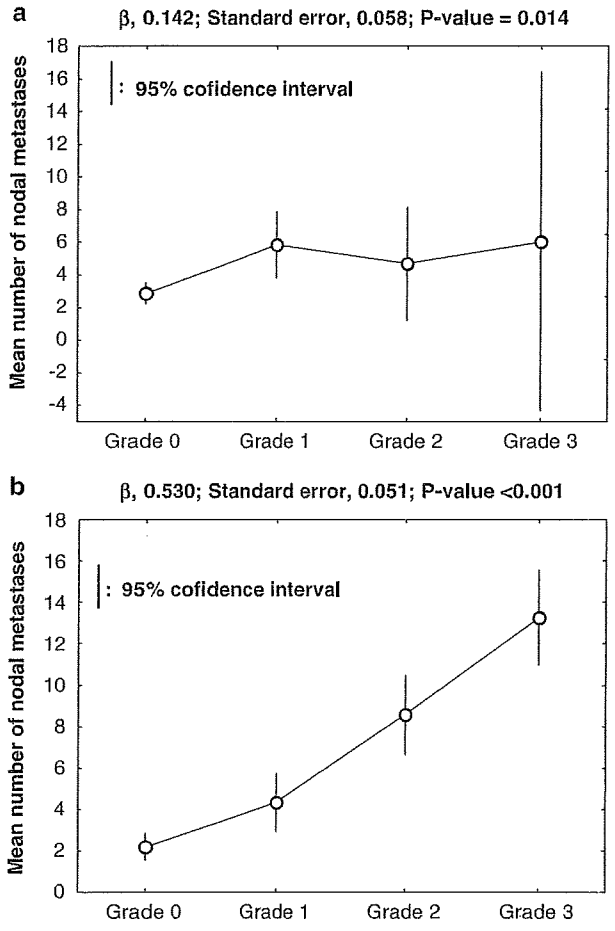

Figure 2 Graphs showing associations between mean nodal metastasis values and the grades of lymph vessel tumor emboli in the biopsy specimens (**a**) and in the surgical specimens (**b**). The mean number of nodal metastases increases significantly with the grade of lymph vessel tumor emboli in the biopsy specimens and in the surgical specimens.

variate analyses were then entered together into the multivariate analyses according to nodal status. As the eight factors were examined using both biopsy specimens obtained before neoadjuvant therapy and surgical specimens obtained after neoadjuvant chemotherapy, to accurately assess the prognostic value of each of these factors in multivariate analyses, their mutual influence on outcome was avoided by conducting separate analyses of the prognostic predictive power of the findings in the biopsy specimens obtained before neoadjuvant therapy and the surgical specimens obtained after neoadjuvant therapy (model 1, factors examined based on biopsy specimens obtained before neoadjuvant therapy; model 2, factors examined based on surgical specimens obtained after neoadjuvant therapy). The case-wise and step-down method was applied until all the remaining factors were significant at a *P*-value below 0.05. As there were fewer than 10 tumor deaths among the patients who did not have nodal metastasis, we were unable to perform multivariate analyses for tumor death in this groups.

Table 1 Association between grading system for lymph vessel tumor emboli and the Allred scores for p53 in stroma-invasive tumor cells, the Allred scores for p53 in tumor-stromal fibroblasts and the Allred scores for p53 in lymph vessel tumor emboli assessed in the surgical specimens

	Grades of lymph vessel tumor emboli				
Case ($n=271$)	*Grade 0* 191	*Grade 1* 42	*Grade 2* 22	*Grade 3* 16	*P-value*
Allred scores for p53 in stroma-invasive tumor cells					
0 or 2 or 3	63 (33)	14 (32)	6 (27)	0	0.001
4–6	75 (39)	22 (54)	9 (41)	3 (19)	
7 or 8	53 (28)	6 (14)	7 (32)	13 (81)	
Allred scores for p53 in tumor-stromal fibroblasts					
0 or 2	110 (58)	27 (64)	6 (27)	1 (6)	<0.001
3	26 (13)	6 (14)	2 (9)	5 (31)	
4–8	55 (29)	9 (22)	14 (64)	10 (63)	
Allred scores for p53 in lymph vessel tumor emboli					
0 or 2 or 3		6 (55)	2 (50)	1 (9)	0.005
4–6		2 (18)	0	0	
7 or 8		3 (27)	2 (50)	10 (91)	

Survival curves were drawn by the Kaplan–Meier method. All analyses were performed with Statistica/Windows software (StatSoft, Tulsa, OK, USA).

Results

Associations Between the Lymph Vessel Tumor Embolus Grades and Factors

Although the lymph vessel tumor embolus grades based on the biopsy specimens and based on the surgical specimens were significantly associated with the increases in mean number of nodal metastases (Figure 2), the value of β for the correlation between lymph vessel tumor embolus grades in the surgical specimens and mean number of nodal metastases was higher than between the lymph vessel tumor embolus grades in the biopsy specimens and the mean number of nodal metastases.

The results of the univariate analyses showed that the lymph vessel tumor embolus grades assessed in the surgical specimens were significantly associated with the Allred scores for p53 in stroma-invasive tumor cells and in tumor-stromal fibroblasts assessed in the surgical specimens (Table 1) and that they were also significantly inversely associated with Allred score for estrogen receptor in stroma-invasive tumor cells assessed in the surgical specimens in the univariate analyses (data not shown). There was no significant association between lymph vessel tumor embolus grades in the surgical specimens and progesterone receptor in stroma-invasive tumor cells in the surgical specimens, and between lymph vessel tumor embolus grades in the surgical specimens and HER2 category in tumor cells in the surgical specimens (data not shown). The Allred scores for p53 in lymph vessel tumor emboli

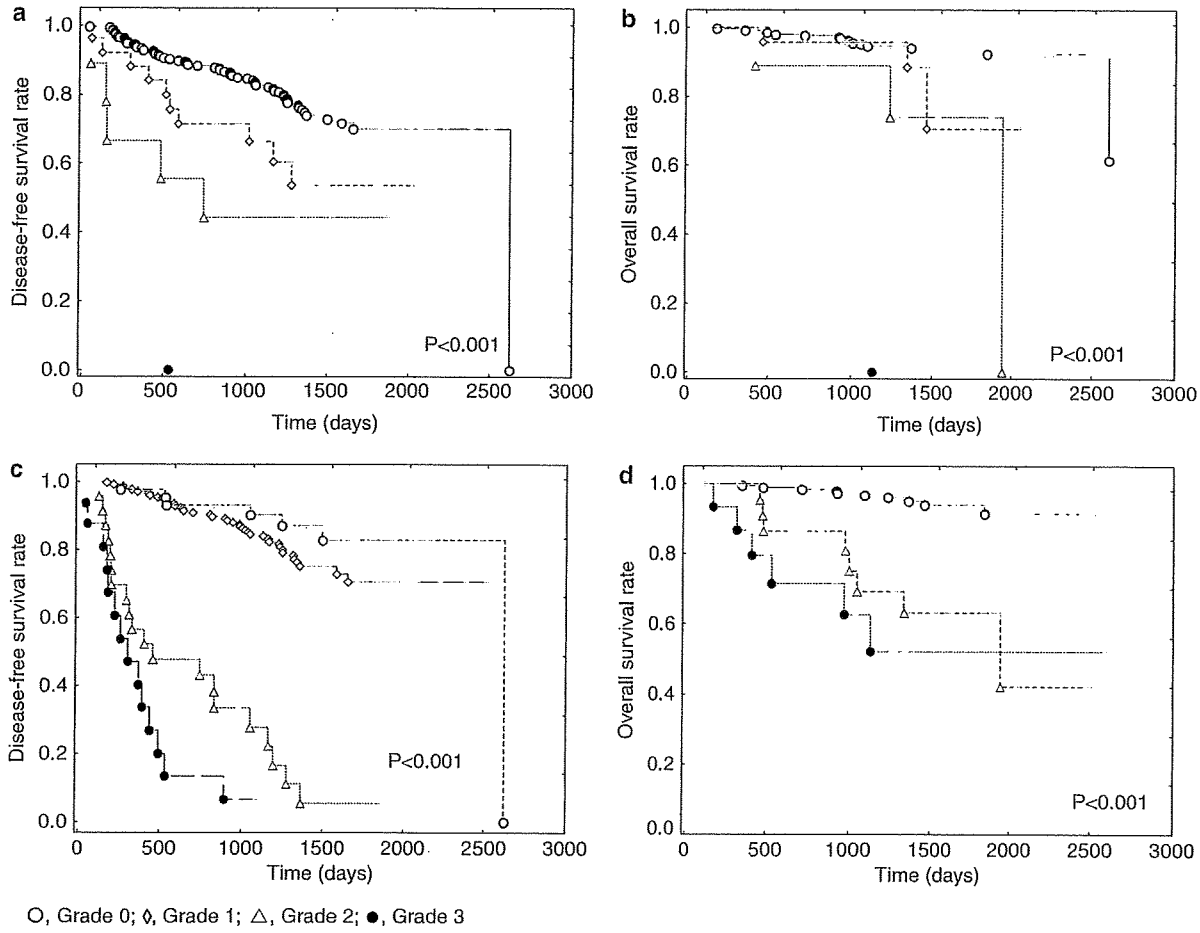

Figure 3 Disease-free survival curves (**a** and **c**) and overall survival curves (**b** and **d**) of all of the invasive ductal carcinoma (IDC) patients who received neoadjuvant therapy as a whole. (**a** and **b**) The disease-free survival time and the overall survival time of the IDC patients classified by grade of lymph vessel tumor emboli in the biopsy specimens obtained before neoadjuvant therapy become significantly shorter as the grades of lymph vessel tumor emboli increased. (**c** and **d**) The disease-free survival time and the overall survival time of the IDC patients classified by the grade of lymph vessel tumor emboli in the surgical specimens become significantly shorter as the grades of lymph vessel tumor emboli increased. None of the IDC patients had grade 1 lymph vessel tumor emboli show tumor-related death.

assessed in the surgical specimens were significantly associated with the grades of the lymph vessel tumor emboli assessed in the surgical specimens (Table 1), but there were no significant associations between the Allred scores for estrogen receptor or progesterone receptor in lymph vessel tumor emboli, or the HER2 categories in the lymph vessel tumor emboli and grades of lymph vessel tumor embolus assessed in the surgical specimens (data not shown).

In our previous study, although the multivariate analysis clearly showed that negative nodal status and HER2 category 3 in tumor cells were significantly associated with pathological complete response,[8] the lymph vessel tumor embolus grades based on the biopsy specimens were not significantly associated with pathological complete response in the univariate analysis (data not shown).

Factors Significantly Associated with Outcome

The univariate analyses of all of the cases as a whole showed that the lymph vessel tumor embolus grades in the biopsy specimens (Figures 3a and b) and the surgical specimens (Figures 3c and d) were significantly associated with tumor recurrence and tumor-related death (Table 2). In the multivariate analyses using model 1, UICC pTNM-pN1, N2, and N3 categories significantly increased the hazard rates for tumor recurrence, and UICC pTNM-pN2 and N3 also significantly increased the hazard rates for tumor-related death (data not shown). The Allred score of 3 for p53 in tumor-stromal fibroblasts and Allred scores of 4–8 for p53 in tumor-stromal fibroblasts significantly increased the hazard rates for tumor recurrence, and lymph vessel tumor embolus grades 2 and 3 also significantly increased the hazard rate

Table 2 Outcome rates of patients with invasive ductal carcinoma according to grade of lymph vessel tumor emboli, and according to nodal status

	Grade of lymph vessel tumor emboli							
Grade	*Assessed in the biopsy specimens*				*Assessed in the surgical specimens*			
	Cases	*TRR (%)*	*MR (%)*	P-*value*	*Cases*	*TRR (%)*	*MR (%)*	P-*value*
Invasive ductal carcinoma patients as a whole								
0	260	61 (23)	16 (6)	TRR <0.001	199	42 (21)	10 (5)	TRR <0.001
1	26	10 (38)	3 (12)	MR <0.001	43	7 (16)	0	MR <0.001
2	9	5 (56)	3 (33)		23	20 (87)	8 (35)	
3	1	1 (100)	1 (100)		16	14 (88)	6 (38)	
Total	296	77	23		281	83	24	
Invasive ductal carcinoma patients who did not have nodal metastasis								
0	113	10 (9)	3 (3)	TRR 0.003	90	12 (13)	2 (2)	TTR 0.010
1	12	4 (33)	0	MR 0.130	7	0	0	MR 0.006
2	2	1 (50)	1 (50)		3	3 (100)	2 (67)	
3	0				0			
Total	127	15	4		100	15	4	
Invasive ductal carcinoma patients who had nodal metastasis								
0	147	51 (35)	13 (9)	TTR 0.007	109	30 (28)	8 (7)	TTR <0.001
1	14	6 (43)	3 (21)	MR 0.001	36	7 (19)	0	MR <0.001
2	7	4 (57)	2 (29)		20	17 (85)	6 (30)	
3	1	1 (100)	1 (100)		16	14 (88)	6 (38)	
Total	169	62	19		181	68	20	

MR, mortality rate; TRR, tumor recurrence rate.

for tumor recurrence in the multivariate analyses (data not shown). Allred scores of 7 or 8 for estrogen receptors in tumor cells significantly decreased the hazard rate for tumor-related death, and HER2 category 3 in tumor cells significantly increased the hazard rate for tumor-related death in the multivariate analyses (data not shown). When model 2 was used, lymph vessel tumor embolus grade 2 and lymph vessel tumor embolus grade 3 significantly increased the hazard rates for tumor recurrence and tumor-related death in the multivariate analyses (data not shown). The Allred score of 3 in tumor-stromal fibroblasts, Allred scores of 4–8 for p53 in tumor-stromal fibroblasts, and histological grade 3 significantly increased the hazard rates for tumor recurrence, and the Allred scores of 4–8 in tumor-stromal fibroblasts and histological grade 3 also significantly increased the hazard rate for tumor-related death in the multivariate analyses (data not shown). Residual invasive tumor size >50 mm significantly increased the hazard rate for tumor recurrence and the presence of skin invasion significantly increased the hazard rate for tumor-related death in the multivariate analyses (data not shown).

In the group of IDC patients without nodal metastasis, the univariate analyses showed that the lymph vessel tumor embolus grades in the biopsy specimens were significantly associated with tumor recurrence, but not with tumor-related death, and that the lymph vessel tumor embolus grades in the surgical specimens were significantly associated with both tumor recurrence and tumor-related death (Table 2). In the multivariate analyses, lymph vessel tumor embolus grades 1 and 2 in the biopsy specimens, Allred scores of 4–8 for p53 in tumor-stromal fibroblasts in the biopsy specimens, and age ≤38 years significantly increased the hazard rates for tumor recurrence in the multivariate analyses (Table 3, model 1), and lymph vessel tumor embolus grade 2 in the surgical specimens, Allred score of 3 for p53 in tumor-stromal fibroblasts in the surgical specimens, and Allred scores of 4–8 for p53 in tumor-stromal fibroblasts in the surgical specimens significantly increased the hazard rates for tumor recurrence in the multivariate analysis (Table 3, model 2).

In the group of IDC patients with nodal metastasis, the univariate analyses showed that the lymph vessel tumor embolus grades in the biopsy specimens and the surgical specimens were significantly associated with tumor recurrence and tumor-related death (Table 2). In the multivariate analyses of model 1, lymph vessel tumor embolus grades 2 and 3, an Allred score of 3 for p53 in tumor-stromal fibroblasts, and Allred scores of 4–8 for p53 in tumor-stromal fibroblasts significantly increased the hazard rate for tumor recurrence, and lymph vessel tumor embolus grade 1 significantly increased the hazard rate for tumor-related death (Table 4). The Allred scores of 7 or 8 for estrogen receptors in tumor cells significantly decreased the hazard rate

Table 3 Multivariate analysis for tumor recurrence in invasive ductal carcinoma patients who did not have nodal metastasis

Factors	*Cases*	*Number of patients (%) Tumor recurrence*			
		Present	*HRs*	*95% CI*	P-*value*
Model 1					
Grading system for lymph vessel tumor emboli					
Grade 0	113	10 (9)	Referent		
Grades 1 and 2	12	4 (33)	4.2	1.3–13.0	0.014
The Allred scores for p53 in tumor-stromal fibroblasts					
0 or 2	40	0	Referent		
3	27	3 (11)	Referent		
4–8	57	12 (21)	3.9	1.1–14.3	0.037
Age (years)					
⩽39	21	7 (33)	Referent		
>39	114	11 (10)	0.3	0.1–0.9	0.040
Model 2					
Grading system for lymph vessel tumor emboli					
Grade 0	90	12 (13)	Referent		
Grade 1	7	0	Referent		
Grade 2	3	3 (100)	10.2	2.5–40.9	0.001
The Allred scores for p53 in tumor-stromal fibroblasts					
0 or 2	64	3 (5)	Referent		
3	12	4 (33)	6.4	1.4–29.6	0.017
4–8	19	7 (37)	9.8	2.2–34.9	0.002

CI, confidence interval; HR, hazard rate.
Model 1: Tumor recurrence was adjusted for grading system for lymph vessel tumor emboli and the Allred scores for p53 in tumor-stromal fibroblasts assessed in biopsy specimen obtained before neoadjuvant therapy, and age.
Model 2: Tumor recurrence was adjusted for grading system for lymph vessel tumor emboli and the Allred scores for p53 in tumor-stromal fibroblasts assessed in surgical specimen obtained after neoadjuvant therapy, and age.

for tumor recurrence, and Allred scores of 3–6 for estrogen receptors in tumor cells significantly decreased the hazard rate for tumor death in the multivariate analyses (Table 4). UICC pN3 category significantly increased the hazard rate for tumor recurrence, and HER2 category 3 in tumor cells, histological grade 3, and absence of adjuvant therapy significantly increased the hazard rates for tumor-related death in the multivariate analyses (Table 4). In model 2, lymph vessel tumor embolus grade 2, lymph vessel tumor embolus grade 3, Allred scores of 4–8 for p53 in tumor-stromal fibroblasts, and histological grade 3 significantly increased the hazard rates for tumor recurrence and tumor-related death in the multivariate analyses (Table 4). Residual invasive tumor size >50 mm and Allred scores of 7 or 8 for p53 in tumor cells significantly increased the hazard rates for tumor recurrence, and the presence of skin invasion significantly increased the hazard rate for tumor-related death in the multivariate analysis (Table 4).

Discussion

The results of this study clearly showed significant associations between increases in grade of lymph vessel tumor embolus assessed in the biopsy specimens and surgical specimens and the number of nodal metastases. We have also found a significant association between grade of lymph vessel tumor embolus and number of nodal metastases in a different no-neoadjuvant therapy IDC group in another study.[6] Thus, the grading system for lymph vessel tumor embolus can be concluded to be a very useful histological grading system for accurately predicting lymph node metastasis by IDCs in the no-neoadjuvant therapy group and in the neoadjuvant therapy group.

In a previous study, we found that the grading system for lymph vessel tumor emboli can be used to classify IDC patients with lymph vessel invasion into a low-, intermediate-, and high-risk groups for outcome, and that IDCs with grade 0 lymph vessel tumor embolus and IDCs with grade 1 lymph vessel tumor emboli were almost equally malignant in a different no-neoadjuvant therapy IDC group.[6] Although those findings were clearly confirmed in this study again, the results of this study clearly showed that lymph vessel tumor embolus grade 2 in the surgical specimens was an important outcome-predictive factor for IDC patients independent of nodal status. It can be therefore concluded that lymph vessel tumor embolus grade 2 is an

Table 4 Multivariate analyses for tumor recurrence and tumor-related death in invasive ductal carcinoma patients who had nodal metastasis

Factors	*Cases*	*Number of patients (%)*			
		Tumor recurrence		*Tumor-related death*	
		Present	*HRs (95% CI)* P-*value*	*Present*	*HRs (95% CI)* P-*value*
Model 1					
Grading system for lymph vessel tumor emboli					
Grade 0	147	51 (35)	Referent	13 (9)	Referent
Grade 1	14	6 (43)	1.8 (0.7–5.0) 0.249	3 (21)	4.3 (1.1–17.7) 0.044
Grades 2 and 3	8	5 (63)	3.6 (1.4–9.5) 0.008	3 (38)	0.5 (0.1–3.3) 0.458
The Allred scores for p53 in tumor-stromal fibroblasts					
0 or 2	47	7 (15)	Referent	0	Referent
3	38	14 (36)	(1.6–9.1) 0.003	6 (16)	Referent
4–8	81	39 (48)	2.4 (1.4–4.1) 0.002	11 (14)	1.8 (0.6–5.7) 0.324
The Allred scores for estrogen receptors in tumor cells					
0 or 2	62	28 (45)	Referent	14 (23)	Referent
3–6	22	11 (50)	1.4 (0.5–3.7) 0.550	3 (14)	0.1 (0.02–0.6) 0.009
7 or 8	82	21 (26)	0.4 (0.2–0.6) <0.001	0	
UICC pN category					
N1	97	27 (28)	Referent	6 (6)	Referent
N2	55	25 (45)	1.7 (0.8–3.5) 0.158	11 (20)	—
N3	31	17 (55)	2.6 (1.4–4.7) 0.002	4 (13)	—
HER2 category in tumor cells					
0 or 1	104	35 (34)	Referent	5 (5)	Referent
2	28	8 (29)	0.6 (0.3–1.4) 0.244	2 (7)	0.6 (0.06–7.1) 0.703
3	35	18 (51)	1.5 (0.7–3.4) 0.317	11 (31)	14.5 (3.9–53.1) <0.001
Histological grade					
1	43	7 (16)	Referent	0	Referent
2	104	46 (44)	2.3 (0.9–5.9) 0.082	13 (13)	Referent
3	22	9 (41)	2.0 (0.6–6.6) 0.281	6 (27)	6.2 (1.8–21.0) 0.003
Adjuvant therapy					
No	36	16 (44)	Referent	7 (19)	Referent
Yes	147	53 (36)	— —	14 (10)	0.2 (0.06–0.7) 0.014
Model 2					
Grading system for lymph vessel tumor emboli					
Grade 0	109	30 (28)	Referent	8 (7)	Referent
Grade 1	36	7 (19)	0.3 (0.1–0.9) 0.027	0	Referent
Grade 2	20	17 (85)	5.7 (2.9–11.0) <0.001	6 (30)	4.2 (1.4–12.6) 0.010
Grade 3	16	14 (88)	6.8 (3.1–14.8) <0.001	6 (38)	8.1 (2.5–25.7) <0.001
The Allred scores for p53 in tumor-stromal fibroblasts					
0 or 2	80	16 (20)	Referent	4 (5)	Referent
3	27	9 (33)	1.4 (0.5–4.0) 0.484	0	Referent
4–8	69	41 (59)	2.5 (1.5–4.3) 0.001	16 (23)	5.2 (1.9–14.4) 0.002

Table 4 Continued

Factors	*Cases*	*Number of patients (%)*			
		Tumor recurrence		*Tumor-related death*	
		Present	*HRs (95% CI)* P-*value*	*Present*	*HRs (95% CI)* P-*value*
Histological grade					
1	43	5 (12)	Referent	0	Referent
2	86	32 (37)	1.9 (0.7–5.7) 0.232	5 (6)	Referent
3	52	31 (60)	2.2 (3.1–14.8) <0.001	15 (29)	5.4 (1.9–15.9) 0.002
Residual invasive tumor size (mm)					
⩽20	42	8 (19)	Referent	3 (7)	Referent
>20–⩽50	92	29 (32)	1.0 (0.4–2.4) 0.943	8 (9)	—
>50	47	31 (66)	3.0 (1.8–5.3) <0.001	9 (19)	—
The Allred scores for p53 in tumor cells					
0 or 2	48	12 (25)	Referent	2 (4)	Referent
3–6	79	25 (32)	1.9 (0.8–4.6) 0.142	6 (8)	3.0 (0.5–17.5) 0.224
7 or 8	48	29 (60)	2.1 (1.1–4.2) 0.023	12 (25)	1.2 (0.2–8.0) 0.817
Skin invasion					
Absent	131	40 (31)	Referent	9 (7)	Referent
Present	50	28 (56)	1.9 (0.9–3.6) 0.068	11 (22)	2.9 (1.1–7.5) 0.025

CI, confidence interval; HR, hazard rate; —, not significant in univariate analysis.
Model 1: Tumor recurrence was adjusted for grading system for lymph vessel tumor emboli, the Allred scores for p53 in tumor-stromal fibroblasts, histological grade, the Allred scores for estrogen receptors in tumor cells, HER2 category in tumor cells, the Allred scores for progesterone receptors, and the Allred scores for p53 in tumor cells assessed in biopsy specimens obtained before neoadjuvant therapy, and UICC pN category assessed in surgical specimens obtained after neoadjuvant therapy and type of neoadjuvant therapy. Tumor-related death was adjusted for grading system for lymph vessel tumor emboli, the Allred scores for p53 in tumor-stromal fibroblasts, histological grade, the Allred scores for estrogen receptors in tumor cells, HER2 category in tumor cells, and the Allred scores for progesterone receptors in tumor cells assessed in biopsy specimens obtained before neoadjuvant therapy, and adjuvant therapy.
Model 2: Tumor recurrence was adjusted for grading system for lymph vessel tumor emboli, the Allred scores for p53 in tumor-stromal fibroblasts, histological grade, residual invasive tumor size, the Allred scores for p53 in tumor cells, skin invasion, the Allred scores for estrogen receptors in tumor cells, HER2 category in tumor cells and UICC pN category assessed in surgical specimens obtained after neoadjuvant therapy, and type of neoadjuvant therapy. Tumor-related death was adjusted for grading system for lymph vessel tumor emboli, the Allred scores for p53 in tumor-stromal fibroblasts, histological grade, residual invasive tumor size, the Allred scores for p53 in tumor cells, skin invasion, the Allred scores for estrogen receptors in tumor cells, and HER2 category in tumor cells assessed in surgical specimens obtained after neoadjuvant therapy, and adjuvant therapy.

important outcome predictor for IDC patients who have received neoadjuvant therapy, the as same as lymph vessel tumor embolus grade 3 is. The results of this study also clearly showed that lymph vessel tumor embolus grades based on biopsy specimens or surgical specimens are a very important outcome-predictive factor for IDC patients who have received neoadjuvant therapy independent of nodal status, but the outcome-predictive power of lymph vessel tumor embolus grade in the surgical specimens was superior to that of lymph vessel tumor embolus grade in the biopsy specimens. Thus, we can conclude that evaluation of lymph vessel tumor embolus grade in surgical specimens should be used to predict outcome.

Although we have already reported that lymph vessel tumor embolus grade is an important outcome predictor for IDC patients who have received neoadjuvant therapy, the outcome-predictive power of the lymph vessel tumor embolus grade for IDC patients who received neoadjuvant therapy and did not have nodal metastasis could not be assessed.[7] This study clearly showed that lymph vessel tumor embolus grades based on biopsy specimens and surgical specimens are very important outcome predictors for IDC patients who have received neoadjuvant therapy and do not have nodal metastasis. Furthermore, the outcome-predictive power of lymph vessel tumor embolus grade is almost the same as that of p53 expression in tumor-stromal fibroblasts, and superior to that of histological grade.

The lymph vessel tumor embolus grading system is therefore concluded to be an excellent histological grading system for accurately predicting the outcome of IDC patients who have received neoadjuvant therapy that is independent of their nodal status.

The results of this study clearly showed that lymph vessel tumor embolus grades are significantly associated with both the Allred scores for p53 in lymph vessel tumor emboli, as well as the Allred scores for p53 in stroma-invasive tumor cells, and in tumor-stromal fibroblasts, this strongly suggesting that p53 protein expression in lymph vessel tumor emboli, in tumor-stromal fibroblasts, and in stroma-invasive tumor cells is a very important key factor for evaluating the malignant potential of IDCs with lymph vessel tumor emboli. Especially, as lymph vessel tumor embolus grades are based on the numbers of mitotic figures and apoptotic figures in tumor cells in lymph vessels, p53 protein expression in lymph vessel tumor embolus probably accelerates the turnover rate of tumor cells comprising lymph vessel tumor emboli, and increases the malignancy of IDCs as lymph vessel tumor embolus grade rises. As we did not investigate for the presence of p53 gene abnormalities, the mechanism that is responsible for the increase in the malignant potential of IDCs according to grades of lymph vessel tumor embolus from the standpoint of p53 gene abnormalities in lymph vessel tumor emboli, as well as in tumor-stromal fibroblasts, or in stroma-invasive tumor cells should be investigated. In addition, as some studies have reported some identifying genes that closely regulate the cell cycle of tumors,[24–26] such genes should be investigated to determine whether they are candidates for p53 in regulating tumor cell cycle of lymph vessel tumor emboli.

In conclusion, the grading system for lymph vessel tumor emboli is significantly associated with nodal metastasis, and is an excellent histological grading system for accurately predicting the outcome of patients with IDC of the breast who received neoadjuvant therapy. Pathologists can most accurately assess the true malignant potential of IDCs by using this grading system as a histological prognostic classification for IDCs of the breast.

Acknowledgement

This study was supported by a Grant-in-Aid for Scientific Research (KAKENHI) (C) (19590378, 21590393) from the Japan Society for the Promotion of Science and was supported in part by a Grant-in-Aid for Cancer Research from the Ministry of Health, Labor and Welfare (20–16, H21-006).

Disclosure/conflict of interest

The authors declare no conflict of interest.

References

1 Lauria R, Perrone F, Carlomagno C, *et al.* The prognostic value of lymphatic and blood vessel invasion in operable breast cancer. Cancer 1995;76:1772–1778.
2 Nime FA, Rosen PP, Tzvi Thaler H, *et al.* Prognostic significance of tumor emboli intramammary lymphatics in patients with mammary carcinoma. Am J Surg Pathol 1977;1:25–30.
3 Hasebe T, Sasaki S, Imoto S, *et al.* Characteristics of tumors in lymph vessels play an important role in the tumor progression of invasive ductal carcinoma of the breast: a prospective study. Mod Pathol 2002; 15:904–913.
4 Hoshida T, Isaka N, Hagendoorn J, *et al.* Imaging steps of lymphatic metastasis reveals that vascular endothelial growth factor-C increases metastasis by increasing delivery of cancer cells to lymph nodes: therapeutic implications. Cancer Res 2006;66:8065–8075.
5 Yamauchi C, Hasebe T, Iwasaki M, *et al.* Accurate assessment of lymph vessel tumor emboli in invasive ductal carcinoma of the breast according to tumor areas, and their prognostic significance. Hum Pathol 2007;38:247–259.
6 Hasebe T, Yamauchi C, Iwasaki M, *et al.* Grading system for lymph vessel tumor emboli for prediction of the outcome of invasive ductal carcinoma of the breast. Hum Pathol 2008;39:427–436.
7 Tamura N, Hasebe T, Okada N, *et al.* Tumor histology in lymph vessels and lymph nodes for the accurate prediction of outcome among breast cancer patients treated with neoadjuvant chemotherapy. Cancer Sci 2009;100:1823–1833.
8 Hasebe T, Tamura N, Okada N, *et al.* p53 expression in tumor stromal fibroblasts is closely associated with the nodal metastasis and the outcome of patients with invasive ductal carcinoma who received neoadjuvant therapy. Hum Pathol 2009;41:262–270.
9 Sobin LH, Wittekind Ch. UICC International Union Against Cancer. TNM classification of malignant tumors. In: Sobin LH and Wittekind Ch (eds). 6th edn. Wiley-Liss: Geneva, 2002, pp 131–141.
10 Bloom HJG, Richardson WW. Histological grading and prognosis in breast cancer. Br J Cancer 1957; 11:359–377.
11 Gilchrist KW, Gray R, Fowble B, *et al.* Tumor necrosis is a prognostic predictor for early recurrence and death in lymph node-positive breast cancer: a 10-year follow-up study of 728 eastern cooperative oncology group patients. J Clin Oncol 1993;11:1929–1935.
12 Hasebe T, Tsuda H, Hirohashi S, *et al.* Fibrotic focus in infiltrating ductal carcinoma of the breast: a significant histopathological prognostic parameter for predicting the long-term survival of the patients. Breast Cancer Res Treat 1998;49:195–208.
13 Hasebe T, Sasaki S, Imoto S, *et al.* Prognostic significance of fibrotic focus in invasive ductal carcinoma of the breast: a prospective observational study. Mod Pathol 2002;15:502–516.
14 Fisher B. Biological and clinical considerations regarding the use of surgery and chemotherapy in the treatment of primary breast cancer. Cancer 1977; 40:574–587.
15 Fisher B. Adjuvant chemotherapy in the primary management of breast cancer. Med Clin North Am 1977;61:953–965.

16 Fukunaga M. Expression of D2-40 in lymphatic endothelium of normal tissues and in vascular tumours. Histopathology 2005;46:396–402.
17 Niakosari F, Kahn HJ, Marks A, *et al.* Detection of lymphatic invasion in primary melanoma with monoclonal antibody D2-40: a new selective immunohistochemical marker of lymphatic endothelium. Arch Dermatol 2005;141:440–444.
18 Allred DC, Harvey JM, Berardo MD, *et al.* Prognostic and predictive factors in breast cancer by immunohistochemical analysis. Mod Pathol 1998;11:155–168.
19 Harvey JM, Clark GM, Osborne K, *et al.* Estrogen receptor status by immunohistochemistry is superior to the ligand-binding assay for predicting response to adjuvant endocrine therapy in breast cancer. J Clin Oncol 1999;17:1474–1481.
20 Mohsin S, Weiss H, Havighurst T, *et al.* Progesterone receptor by immunohistochemistry and clinical outcome in breast cancer: a validation study. Mod Pathol 2004;17:1545–1554.
21 Badve SS, Baehner FL, Gray RP, *et al.* Estrogen- and progesterone-receptor status in ECOG2197: comparison of immunohistochemistry by local and central laboratories and quantitative reverse transcription polymerase chain reaction by central laboratory. J Clin Oncol 2008;26:2473–2481.
22 Allred DC, Clark GM, Elledge R, *et al.* Association of p53 protein expression with tumor cell proliferation rate and clinical outcome in node-negative breast cancer. J Natl Cancer Inst 1993;85:200–206.
23 Wolff AC, Hammond ME, Schwartz JN, *et al.* American Society of Clinical Oncology/College of American Pathologists guideline recommendations for human epidermal growth factor receptor 2 testing in breast cancer. Arch Pathol Lab Med 2007;131:18–43.
24 Westbrook L, Manuvakhova M, Kern FG, *et al.* Cks1 regulates cdk1 expression: a novel role during mitotic entry in breast cancer cells. Cancer Res 2007;67:11393–11401.
25 Nakamura Y, Tanaka F, Haraguchi N, *et al.* Clinicopathological and biological significance of mitotic centromere-associated kinesin overexpression in human gastric cancer. Br J Cancer 2007;97:543–549.
26 Budhram-Mahadeo VS, Irshad S, Bowen S, *et al.* Proilferation-associated Brn-3b transcription factor can activate cyclin D1 expression in neuroblastoma and breast cancer cells. Br J Cancer 2008; 27:145–154.

Original article

Endoscopic resection of early gastric cancer treated by guideline and expanded National Cancer Centre criteria

T. Gotoda[1], M. Iwasaki[2], C. Kusano[1], S. Seewald[3] and I. Oda[1]

[1]Endoscopy Division and [2]Epidemiology and Prevention Division, Research Centre for Cancer Prevention and Screening, National Cancer Centre, Tokyo, and [3]Gastroenterology Centre, Klink Hirslanden, Zurich, Switzerland

Correspondence to: Dr T. Gotoda, Endoscopy Division, National Cancer Centre Hospital, 5-1-1, Tsukiji, Chuo-ku, Tokyo 104-0045, Japan (e-mail: tgotoda@ncc.go.jp)

Background: Criteria for endoscopic resection in patients with early gastric cancer (EGC) have been expanded recently by the National Cancer Centre (NCC). This study compared long-term outcomes in patients with EGC who underwent endoscopic treatment according to guideline criteria with those treated according to expanded criteria.

Methods: Baseline and outcome data from patients undergoing curative endoscopic resection for EGC between January 1999 and December 2005 were collected from electronic medical records. Survival time hazard ratios and 95 per cent confidence intervals were calculated using the Cox proportional hazards model.

Results: Of 1485 patients who had a curative resection, 635 (42·8 per cent) underwent resection according to traditional criteria and 625 (42·1 per cent) according to expanded criteria. There was no significant difference in overall survival between the groups.

Conclusion: Patients who have treatment following the expanded criteria have similar long-term survival and outcomes to those treated according to guideline criteria.

Paper accepted 22 January 2010

Published online in Wiley InterScience (www.bjs.co.uk). **DOI:** 10.1002/bjs.7033

Introduction

In Japan, endoscopic mucosal resection (EMR) has been the treatment of choice for small early gastric cancer (EGC) for the past two decades[1,2]. Owing to the technical limitations of EMR, traditional indications for endoscopic resection of EGC according to the Gastric Cancer Treatment Guidelines of the Japanese Gastric Cancer Association (JGCA) were restricted to resection of small intramucosal EGCs (smaller than 20 mm) with intestinal-type histology and no ulceration.

The low risk of lymph node involvement in EGC confined to the superficial layers of the submucosa indicated that cure can be achieved by local resection, even of lesions larger than 20 mm, as long as the lesion is removed *en bloc*[3]. Endoscopic submucosal dissection (ESD) has become established as a technique that allows *en bloc* resection regardless of size. Revised criteria were proposed by the National Cancer Centre (NCC) in Tokyo (from January 1999) to expand the indications for endoscopic treatment and avoid unnecessary radical surgery, which until recently was the 'gold standard' for larger lesions[4,5].

This study compared the long-term outcome of patients with EGC who underwent endoscopic treatment based on either guideline of JGCA criteria or expanded NCC criteria.

Methods

Consecutive patients who had endoscopic resection for EGC between January 1999 and December 2005 were studied. Informed consent was obtained from all patients in accordance with the institutional protocol. The procedure was carried out under conscious sedation using a combination of midazolam and pentazocine. Patients who were assessed histologically as having had a non-curative resection owing to positive lateral margins and/or deep submucosal invasion, regardless of positive vertical margins and/or lymphatic–vascular infiltration and/or diffuse-type histology, and those who had undergone endoscopic

resection as a palliative treatment for advanced cancer were excluded.

Curability was based on the histological criteria for curative endoscopic resection (*Table 1*) according to the Japanese Classification of Gastric Carcinoma[6]. Pathological assessment of the resected specimen included: size, location, macroscopic appearance, presence of ulceration, histological type, depth of invasion, lymphatic and vascular involvement, and resection margin status. Tumours smaller than 20 mm without ulceration were included in the JGCA criteria group and those larger than 20 mm in the NCC expanded criteria group. Patients with multiple EGCs were analysed as a separate group.

Baseline and outcome data were collected from electronic medical records. Incomplete and missing data were retrieved from different sources such as telephone contact with patients, family and referring physicians, and checked with statistical data kept by the local government registry.

All patients with curative resection who met JGCA criteria were followed up by annual upper gastrointestinal surveillance endoscopy to identify local recurrence and/or metachronous gastric cancer. Patients who met NCC criteria were additionally followed by thoracic and abdominal computed tomography and/or endoscopic ultrasonography every 6 months. Patients were followed from the date of first treatment until 31 July 2007.

Statistical analysis

Survival time was calculated as the interval between the date of the first treatment and the date of death or the last date confirmed as alive for survivors. Survival curves were calculated using the Kaplan–Meier method. To compare overall survival by treatment method, a Cox proportional hazards model was used to estimate hazard ratios and 95 per cent confidence intervals (c.i.). Age, sex and past history of cancer were included as co-variables in the multivariable analyses. All P values reported are two sided and $P < 0{\cdot}050$ was considered statistically significant.

Table 1 Histological criteria for curative endoscopic resection

Factors for no risk of lymph node metastasis
Intestinal-type histology
No lymphatic or vascular infiltration
Intramucosal cancer regardless of tumour size without ulcer finding
or intramucosal cancer less than 30 mm in size with ulcer finding
or minute submucosal invasive cancer (sm1) less than 30 mm in size
Factors for resection margin
Tumour-free horizontal margin
Tumour-free vertical margin

Statistical analyses were performed with SAS® software version 9.1 (SAS Institute, Cary, North Carolina, USA).

Results

Some 1786 lesions were resected curatively among 1485 patients; 635 patients (42·8 per cent) were treated according to the guideline of JGCA criteria and 625 (42·1 per cent) in accordance with the expanded NCC criteria; 225 patients (15·2 per cent) had multiple EGCs with both criteria. Baseline characteristics by treatment allocation are shown in *Table 2*.

Follow-up was complete for all 1485 patients, with a median observation period of 44·1 months. During follow-up, 77 patients died (5·2 per cent). Only one patient treated according to JGCA criteria died from metachronous invasive gastric cancer, which was detected 5 years later. Locally recurrent gastric cancer was found in another patient who underwent piecemeal endoscopic resection. This patient underwent ESD for local recurrence 18 months after the first endoscopic resection and was alive with no evidence of recurrence after 57 months. There was

Table 2 Baseline patient characteristics by treatment group

	JGCA criteria ($n = 635$)	NCC criteria ($n = 625$)	Multiple cancers ($n = 225$)
Mean age (years)	66·4	66·5	68·6
Men	479 (75·4)	505 (80·8)	180 (80·0)
Past history of cancer	154 (24·3)	87 (13·9)	95 (42·2)
Mean tumour size (mm)	10·8	23·8	12·4

JGCA, Japanese Gastric Cancer Association; NCC, National Cancer Centre.

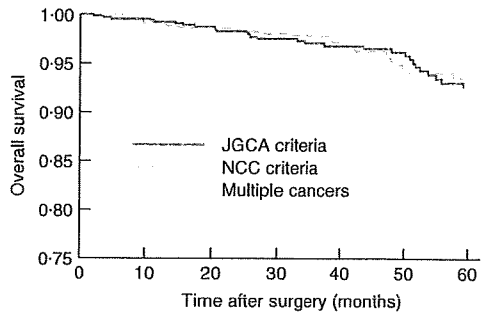

No. at risk							
JGCA criteria	635	631	584	455	346	264	186
NCC criteria	625	621	559	433	314	242	156
Multiple cancers	225	223	210	180	156	126	89

Fig. 1 Survival by treatment group. JGCA, Japanese Gastric Cancer Association; NCC, National Cancer Centre

Table 3 Hazard ratio for all-cause mortality according to treatment group

	No. of deaths	5-year survival rate (%)	Hazard ratio	
			Crude	Adjusted*
JGCA criteria	36	92·4	1·00	1·00
NCC expanded criteria	31	93·4	0·93 (0·57, 1·50)	1·10 (0·67, 1·81)
Multiple cancers	10	95·6	0·63 (0·31, 1·26)	0·46 (0·23, 0·94)

Values in parentheses are 95 per cent confidence intervals. JGCA, Japanese Gastric Cancer Association; NCC, National Cancer Centre. *Multivariable Cox proportional hazards model, adjusted for age, sex and past history of cancer.

no significant difference in the rate of local and/or systemic recurrence between the JGCA and the NCCH groups.

Survival curves are shown in *Fig. 1*. The 5-year survival rate was 92·4 per cent in the JGCA group, 93·4 per cent in the NCCH group and 95·6 per cent among those with multiple cancers. There was no significant difference in overall survival (*Table 3*). In multivariable analysis, the hazard ratio for survival of patients in the NCC group compared with those in the JGCA group was 1·10 (95 per cent c.i. 0·67 to 1·81).

Discussion

Radical surgery with complete removal of first- and second-tier lymph nodes is accepted as a standard treatment for patients with EGC. A 5-year survival rate of around 90 per cent has been achieved in oriental and Western patients[7–9]. In patients with cancer limited to the mucosa, the incidence of lymph node metastasis is less than 3 per cent. This risk increases to 20 per cent when the cancer invades the submucosa[10].

Radical surgery may not be not the optimal treatment approach in all patients with EGC because it carries a significant risk of morbidity and mortality, and is associated with a significant reduction in quality of life[11–13]. Patients with no risk of lymph node metastasis can be treated safely by endoscopic resection[14].

Accepted indications for EMR of ECG have been (1) well differentiated elevated cancers less than 2 cm in diameter and (2) small (maximum 1 cm) depressed lesions without ulceration. These indications were established because of the technical limitations of EMR. In larger lesions, EMR has a high risk of recurrence as a result of incomplete resection when piecemeal EMR is used for larger lesions[15]. Specimens obtained by piecemeal EMR are difficult to analyse and there is a high risk of inadequate histological staging[16]. From a histological point of view, *en bloc* removal should be considered essential for endoscopic resection of larger lesions to ensure accurate histological staging. The treatment strategy for EGC has been revolutionized recently by the ESD procedure. This method is superior to other endoscopic techniques used for EGC as it makes *en bloc* resection possible, allowing precise histological staging and minimizing recurrence risk compared with standard EMR techniques[17].

Kojima and colleagues[18] have reviewed the outcomes of EMR from 12 major institutions in Japan. Long-term outcomes after EMR for small differentiated mucosal EGC less than 2 cm in diameter have been reported to be comparable to those following gastrectomy[19], but the long-term outcome of endoscopic resection of large EGCs has not been reported.

The present study has demonstrated that there is no difference in 5-year survival and local and/or systemic recurrence rates between patients treated according to JGCA or NCC criteria. The hazard ratio for overall survival showed no significant difference between the two groups.

Final staging can be carried out accurately only by formal histological analysis, especially with regard to potential lymphovascular infiltration. Therefore, *en bloc* resection is a prerequisite for accurate staging and prediction of a patient's risk of lymph node metastasis.

Expanded NCC criteria for patients with EGC are safe and practicable. As a result of the ability to achieve *en bloc* resection by ESD, more patients may benefit from endoscopic resection, further reducing the need for radical surgery.

Acknowledgements

The authors declare no conflict of interest.

References

1 Takekoshi T, Baba Y, Ota H, Kato Y, Yanagisawa A, Takagi K *et al.* Endoscopic resection of early gastric carcinoma: results of a retrospective analysis of 308 cases. *Endoscopy* 1994; **26**: 352–358.
2 Rembacken BJ, Gotoda T, Fujii T, Axon AT. Endoscopic mucosal resection. *Endoscopy* 2001; **33**: 709–718.

3 Gotoda T, Sasako M, Ono H, Katai H, Sano T, Shimoda T. Evaluation of the necessity of gastrectomy with lymph node dissection for patients with submucosal invasive gastric cancer. *Br J Surg* 2001; **88**: 444–449.
4 Gotoda T, Yanagisawa A, Sasako M, Ono H, Nakanishi Y, Shimoda T *et al.* Incidence of lymph node metastasis from early gastric cancer: estimation with a large number of cases at two large centers. *Gastric Cancer* 2000; **3**: 219–225.
5 Soetikno R, Kaltenbach T, Yeh R, Gotoda T. Endoscopic mucosal resection for early cancers of the upper gastrointestinal tract. *J Clin Oncol* 2005; **23**: 4490–4498.
6 Japanese Gastric Cancer Association. Japanese classification of gastric carcinoma – 2nd English edition. *Gastric Cancer* 1998; **1**: 10–24.
7 Sano T, Sasako M, Kinoshita T, Maruyama K. Recurrence of early gastric cancer. Follow-up of 1475 patients and review of Japanese literature. *Cancer* 1993; **72**: 3174–3178.
8 Sue-Ling HM, Martin I, Griffith J, Ward DC, Quirke P, Dixon MF *et al.* Early gastric cancer: 46 cases treated in one surgical department. *Gut* 1992; **33**: 1318–1322.
9 Everett SM, Axon AT. Early gastric cancer in Europe. *Gut* 1997; **41**: 142–150.
10 Sano T, Kobori O, Muto T. Lymph node metastasis from early gastric cancer: endoscopic resection of tumour. *Br J Surg* 1992; **79**: 241–244.
11 Sasako M. Risk factors for surgical treatment in the Dutch Gastric Cancer Trial. *Br J Surg* 1997; **84**: 1567–1571.
12 Bonenkamp JJ, Songun I, Hermans J, Sasako M, Welvaart K, Plukker JT *et al.* Randomised comparison of morbidity after D1 and D2 dissection for gastric cancer in 996 Dutch patients. *Lancet* 1995; **345**: 745–748.
13 Bonenkamp JJ, Hermans J, Sasako M, van de Velde CJ, Welvaart K, Songun I *et al.* Extended lymph-node dissection for gastric cancer. *N Engl J Med* 1999; **340**: 908–914.
14 Tsujitani S, Oka S, Saito H, Kondo A, Ikeguchi M, Maeta M *et al.* Less invasive surgery for early gastric cancer based on the low probability of lymph node metastasis. *Surgery* 1999; **125**: 148–154.
15 Tanabe S, Koizumi W, Mitomi H, Nakai H, Murakami S, Nagaba S *et al.* Clinical outcome of endoscopic aspiration mucosectomy for early stage gastric cancer. *Gastrointest Endosc* 2002; **56**: 708–713.
16 Korenaga D, Orita H, Maekawa S, Maruoka A, Sakai K, Ikeda T *et al.* Pathological appearance of the stomach after endoscopic mucosal resection for early gastric cancer. *Br J Surg* 1997; **84**: 1563–1566.
17 Oka S, Tanaka S, Kaneko I, Mouri R, Hirata M, Kawamura T *et al.* Advantage of endoscopic submucosal dissection compared with EMR for early gastric cancer. *Gastrointest Endosc* 2006; **64**: 877–883.
18 Kojima T, Parra-Blanco A, Takahashi H, Fijita R. Outcome of endoscopic mucosal resection for early gastric cancer: review of the Japanese literature. *Gastrointest Endosc* 1998; **48**: 550–554.
19 Uedo N, Iishi H, Tatsuta M, Ishihara R, Higashino K, Takeuchi Y *et al.* Long term outcomes after endoscopic mucosal resection for early gastric cancer. *Gastric Cancer* 2006; **9**: 88–92.

W166–W169 Nucleic Acids Research, 2009, Vol. 37, Web Server issue *Published online 4 June 2009*
doi:10.1093/nar/gkp483

Gendoo: Functional profiling of gene and disease features using MeSH vocabulary

Takeru Nakazato[1,2,*], Hidemasa Bono[1], Hideo Matsuda[2] and Toshihisa Takagi[1]

[1]Database Center for Life Science (DBCLS), Research Organization of Information and Systems (ROIS), Faculty of Engineering Building 12, The University of Tokyo, 2-11-16 Yayoi, Bunkyo-ku, Tokyo 113-0032 and [2]Department of Bioinformatic Engineering, Graduate School of Information Science and Technology, Osaka University, 1-3 Machikaneyama, Toyonaka, Osaka 560-8531, Japan

Received February 15, 2009; Revised April 27, 2009; Accepted May 19, 2009

ABSTRACT

Genome-wide data enables us to clarify the underlying molecular mechanisms of complex phenotypes. The Online Mendelian Inheritance in Man (OMIM) is a widely employed knowledge base of human genes and genetic disorders for biological researchers. However, OMIM has not been fully exploited for omics analysis because its bibliographic data structure is not suitable for computer automation. Here, we characterized diseases and genes by generating feature profiles of associated drugs, biological phenomena and anatomy with the MeSH (Medical Subject Headings) vocabulary. We obtained 1 760 054 pairs of OMIM entries and MeSH terms by utilizing the full set of MEDLINE articles. We developed a web-based application called Gendoo (gene, disease features ontology-based overview system) to visualize these profiles. By comparing feature profiles of types 1 and 2 diabetes, we clearly illustrated their differences: type 1 diabetes is an autoimmune disease (*P*-value = 4.55×10^{-5}) and type 2 diabetes is related to obesity (*P*-value = 1.18×10^{-15}). Gendoo and the developed feature profiles should be useful for omics analysis from molecular and clinical viewpoints. Gendoo is available at http://gendoo.dbcls.jp/.

INTRODUCTION

The major aims of omics analysis are to identify disease-relevant genes and to understand their mechanisms. Genome sequences and transcriptomics provide large amounts of data, and researchers have attempted to interpret these genetic data in conjunction with clinical phenotypes (1–3). To analyze these data, we can easily obtain gene information such as gene names and genomic location, and their features in the form of Gene Ontology (GO) terms (4) from Entrez Gene (5,6) and Ensembl (7). Additionally, as a disease database, we generally refer to the Online Mendelian Inheritance in Man (OMIM: http://www.ncbi.nlm.nih.gov/omim/) (8,9).

OMIM contains nearly 18 000 detailed entries for human genes and genetic disorders. OMIM is a useful resource for obtaining information about diseases. However, it is difficult to utilize OMIM's data for omics analysis because almost all of its sections are written in natural language, namely English sentences (10). To enable computers to handle OMIM data, certain studies (11–15) have organized OMIM by selecting terms referred to in the Clinical Synopsis (CS) section as keywords. The CS section describes clinical features of disorders and their mode of inheritance such as 'autosomal dominant'. Some of the terms in the CS section for Prader–Willi syndrome (OMIM ID: #176270) are shown in Table 1 as an example. Previous studies (12,14) characterized diseases according to corresponding tissue and etiology with CS terms. By using these terms, researchers do not have to use text mining techniques to automatically extract disease information from OMIM for omics analysis. However, even though OMIM includes detailed biological and genetic descriptions, CS terms are mainly clinical and diagnostic terms so that it is difficult to decipher disease information in conjunction with biological process data such as gene expression data. In addition, CS terms, such as 'Cardiac' and 'Cardiovascular', are ambiguous because the assigned terms are often defined by the author's original description of the cited articles (8).

Here, to organize the disease features referred to in OMIM, we attempted to use the MeSH (Medical Subject Headings) controlled vocabulary (16). MeSH contains >20 000 keywords and hierarchically categorized into 15 concepts including 'disease', 'chemicals and drugs' and 'anatomy'. It is originally curated for indexing MEDLINE articles by National Library of Medicine (NLM). In our previous study (17), to annotate genes from biological viewpoint excluded by GO such as disease and drug fields, we assigned MeSH to each gene by using

*To whom correspondence should be addressed. Tel: +81 3 5841 6754; Fax: +81 3 5841 8090; Email: nakazato@dbcls.rois.ac.jp

Table 1. Symptoms referred to in OMIM Clinical Synopsis section for Prader–Willi syndrome (partial)

Inheritance:
Isolated cases
Growth:
Height
Mean adult male height, 155 cm
Mean adult female height, 147 cm
Steady childhood growth
Weight
Onset of obesity from 6 months to 6 years
Central obesity
Respiratory:
Hypoventilation
Hypoxia
Skeletal:
Osteoporosis
Osteopenia
Endocrine features:
Hyperinsulinemia
Growth hormone deficiency
Hypogonadotropic hypogonadism
Miscellaneous:
Food related behavioral problems include excessive appetite and obsession with eating
Temperature instability
High pain threshold
Molecular basis:
Microdeletion of 15q11 in 70% of patients confirmed by fluorescent in situ hybridization
Remainder of cases secondary to maternal disomy
Rare cases secondary to chromosome translocation

Clinical features of a disorder are listed in the Clinical Synopsis (CS) section of the OMIM database. The CS section mainly describes morphologies and events in clinical and diagnostic fields. Each feature is itemized, but a controlled vocabulary is not used.

Entrez Gene as gene data. In this article, we therefore generated feature profiles of diseases by applying MeSH to OMIM data with the method previously described (17). By comparing these feature profiles of genes developed (17) and diseases derived from this work, we aim to assist to interpret omics data from the molecular and clinical aspects.

METHODS

Data collection

We retrieved OMIM data available in February 2008 by downloading from the National Center for Biotechnology Information (NCBI) FTP site (ftp://ftp.ncbi.nih.gov/repository/OMIM/) and by using the web service with Entrez Programming Utilities (http://eutils.ncbi.nlm.nih.gov/entrez/query/static/eutils_help.html). We obtained MeSH terms (2008 release) from the NLM web site (http://www.nlm.nih.gov/mesh/meshhome.html).

Articles extraction related to each OMIM entry

To generate OMIM–MeSH associations, we need to retrieve articles referred to in each OMIM entry because MeSH terms are not assigned to OMIM entries directly, but to MEDLINE. A schematic view of the pipeline for generating OMIM–MeSH associations is shown in Supplementary Figure S1. We retrieved PubMed IDs (PMIDs) cited in the reference section of OMIM (Supplementary Figure S1a) and extracted OMIM IDs described in the abstracts in MEDLINE (Supplementary Figure S1b). We also retrieved PMIDs by searching PubMed by inputting disease names (Supplementary Figure S1c). One of the problems is that one disease often has many names (18), e.g. 'type 2 diabetes', 'non-insulin dependent diabetes' and 'NIDDM'. Another problem is that the same abbreviation may refer to several diseases, genes and drugs (19); for example, 'EVA' refers to 'enlarged vestibular aqueduct' (disease), 'epithelial V-like antigen' (gene) and 'ethylene vinyl acetate' (chemical). We therefore created abbreviation/long-form pairs for disease names such as 'PWS' and 'Prader–Willi syndrome' and searched MEDLINE for articles co-occurring with both names. Accordingly, we retrieved 426 141 unique OMIM ID and PMID pairs and generated 1 760 054 OMIM–MeSH pairs.

Scoring of associations between OMIM entries and MeSH terms

OMIM contains gene entries as molecular mechanisms and disease entries as their phenotypes (8). These types are indicated by symbols prefixed to the OMIM ID. We divided the OMIM entries into three groups according to these types: sequence known (*, +), locus known (%) and phenotype (#, none). We then calculated *P*-values as a score of OMIM–MeSH pairs in each group. The *P*-value is the probability of the actual or a more extreme outcome under the null-hypothesis. The lower *P*-value means the larger significance of association. We also calculated information gain to rank the associations of the OMIM–MeSH pairs as described in (17). Briefly, information gain refers to the frequency of co-occurrence of a disease name and a MeSH term and also refers to the specificity of the MeSH term.

Data visualization

We updated the web-based software application called Gendoo (gene, disease features ontology-based overview system) to visualize associations between OMIM entries and relevant MeSH terms. It was originally developed to visualize gene–MeSH associations (17). Gendoo accepts OMIM IDs, OMIM titles, Entrez Gene IDs, gene names and MeSH terms as input queries. For disease names, Gendoo currently uses descriptions of 'title' and 'alternative titles; symbols' sections of OMIM, so that not all synonyms are included in the disease name dictionary. We will increase the synonyms by involving the canonical name and synonyms (entry terms) of corresponding MeSH terms, and extracting disease names from MEDLINE and OMIM resources with text mining approach. Gendoo generates high-scoring lists that display relevant MeSH terms for diseases, drugs, biological phenomena and anatomy together with their scores (Supplementary Figure. S2a). These MeSH terms are sorted according to their information gain, and the background color of each association indicates its *P*-value. Gendoo also gives a hierarchical-tree view of MeSH terms associated with diseases of interest by using

JavaScript and cascading style sheet (CSS) resources from the Yahoo! User Interface (YUI) library (http://developer.yahoo.com/yui/) (Supplementary Figure S2b).

RESULTS

Table 2 lists top-three keywords related to Prader–Willi syndrome for the features of the 'Disease', 'Chemicals and Drugs', 'Biological Phenomena' and 'Anatomy' fields. Prader–Willi syndrome results from deletion of paternal copies of the imprinted SNRPN (small nuclear ribonucleoprotein polypeptide N) and necdin genes within chromosome 15 (20). Gendoo shows the keyword phrases clearly reflecting the features of Prader–Willi syndrome, including 'Chromosomes, Human, Pair 15', 'Genomic Imprinting' and 'Ribonucleoproteins, Small Nuclear'. Gendoo illustrates the disease features from not only a clinical perspective, but also a biological one, unlike the symptoms referred to in the CS section shown in Table 1. To retrieve more clinical and diagnostic features with MeSH, we can increase the number of novel associations by using terms from the 'Analytical, Diagnostic and Therapeutic Techniques and Equipment' category of MeSH.

We applied this analysis to types 1 and 2 diabetes (OMIM IDs are %222100 and #125853, respectively). Figure 1 summarizes the feature profiles; type 1 diabetes is closely related to 'Autoimmune Diseases' and 'Spleen' (their P-values are 4.55×10^{-5} and 5.53×10^{-7}, respectively), whereas type 2 diabetes is associated with 'Obesity' (P-value $= 1.18 \times 10^{-15}$) and 'Adipocytes' (P-value $= 5.17 \times 10^{-5}$). Type 1 diabetes is involved in immune systems, and type 2 diabetes is a metabolic disorder (21). This result suggests that the MeSH profiles produced by Gendoo can clarify the differences and similarities in features between OMIM entries.

We provide more practical results shown in Supplementary Table S1.

Table 2. Lists of top-three keywords related to Prader–Willi syndrome

MeSH terms	P-value
Diseases	
Prader–Willi syndrome	0
Angelman syndrome	4.05×10^{-140}
Obesity	6.94×10^{-128}
Chemicals and Drugs	
Human growth hormone	5.86×10^{-68}
Ribonucleoproteins, small nuclear	4.29×10^{-62}
Ghrelin	1.58×10^{-50}
Biological Phenomena	
Chromosomes, human, pair 15	0
Genomic imprinting	2.47×10^{-131}
Obesity	1.69×10^{-121}
Anatomy	
Chromosomes, human, pair 15	0
Chromosomes, human, 13–15	1.25×10^{-30}
Adipose tissue	3.93×10^{-13}

We generated feature profiles by using the MeSH vocabulary. Unlike the symptoms referred to in the CS section of OMIM (Table 1), these profiles give not only clinical, but also biological information about the disease.

The Mendelian Inheritance in Man (MIM) is an excellent knowledge bank that has been annotated by Dr McKusick and his colleagues for >40 years, and its online version, OMIM, is accessible through the internet from NCBI (22). However, its bibliographic data structure has prevented OMIM from being fully exploited for omics analysis. To alleviate this problem, we comprehensively characterized human genes and genetic disorders referred to in OMIM with the MeSH vocabulary, and this will enable researchers to decipher their genome-wide data in conjunction with clinical phenotypes by using Gendoo. For example, the developed feature profiles can be applied to analyses of disease-relevant genes by comparing the similarities among profiles of OMIM entries and groups of genes such as those found in the clustering results of gene expression data. Researchers can also make overviews of features of unfamiliar diseases with Gendoo (Supplementary Table S1c and d).

AVAILABILITY

Gendoo can be openly accessed at http://gendoo.dbcls.jp/. Every association file including Entrez Gene/OMIM IDs, MeSH and their scores is available from the web site. Dictionary files including gene/disease names, synonyms and IDs are also downloadable. These web service and files are freely available under a Creative Commons Attribution 2.1 Japan license (http://creativecommons.org/licenses/by/2.1/jp/deed.en).

CONCLUSIONS

We characterized diseases and genes by generating feature profiles of associated drugs, biological phenomena and anatomy with the MeSH vocabulary and developed a web-based application called Gendoo to visualize these

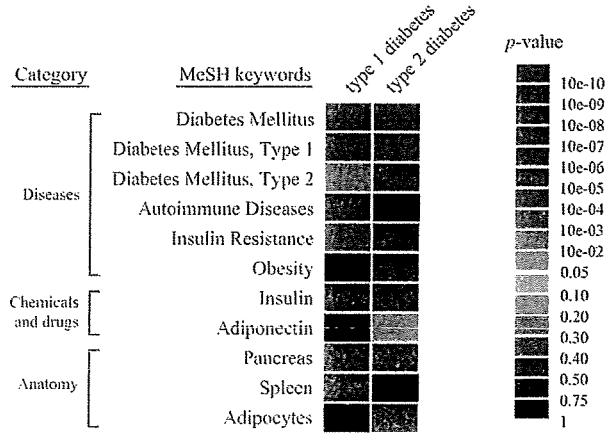

Figure 1. Differences and similarities between feature profiles of types 1 and 2 diabetes. Typical features and scores of types 1 and 2 diabetes are shown. The background colors of each association reflect the P-value. Type 1 diabetes is an autoimmune disorder, whereas type 2 diabetes is a metabolic disorder. These profiles clarify the differences between the features of these diseases.

associations. MeSH profiles illustrate the features of genes and diseases. Comparing profiles emphasizes the differences and similarities between the features of genes and diseases. Gendoo will accelerate the analysis of omics data from biological and clinical perspectives.

SUPPLEMENTARY DATA

Supplementary Data are available at NAR Online.

ACKNOWLEDGEMENTS

We thank Prof. Shoko Kawamoto and Prof. Kousaku Okubo for their helpful discussions.

FUNDING

Integrated Database Project of the Ministry of Education, Culture, Sports, Science and Technology of Japan. Funding for open access charge: Integrated Database Project.

Conflict of interest statement. None declared.

REFERENCES

1. Butte,A.J. and Kohane,I.S. (2006) Creation and implications of a phenome-genome network. *Nat. Biotechnol.*, **24**, 55–62.
2. Perez-Iratxeta,C., Wjst,M., Bork,P. and Andrade,M.A. (2005) G2D: a tool for mining genes associated with disease. *BMC Genet.*, **6**, 45.
3. Perez-Iratxeta,C., Bork,P. and Andrade,M.A. (2002) Association of genes to genetically inherited diseases using data mining. *Nat. Genet.*, **31**, 316–319.
4. Ashburner,M., Ball,C.A., Blake,J.A., Botstein,D., Butler,H., Cherry,J.M., Davis,A.P., Dolinski,K., Dwight,S.S., Eppig,J.T. *et al.* (2000) Gene ontology: tool for the unification of biology. The gene ontology consortium. *Nat. Genet.*, **25**, 25–29.
5. Maglott,D., Ostell,J., Pruitt,K.D. and Tatusova,T. (2007) Entrez Gene: gene-centered information at NCBI. *Nucleic Acids Res.*, **35**, D26–D31.
6. Maglott,D., Ostell,J., Pruitt,K.D. and Tatusova,T. (2005) Entrez Gene: gene-centered information at NCBI. *Nucleic Acids Res.*, **33**, D54–D58.
7. Hubbard,T.J., Aken,B.L., Ayling,S., Ballester,B., Beal,K., Bragin,E., Brent,S., Chen,Y., Clapham,P., Clarke,L. *et al.* (2009) Ensembl 2009. *Nucleic Acids Res.*, **37**, D690–D697.
8. Amberger,J., Bocchini,C.A., Scott,A.F. and Hamosh,A. (2009) McKusick's online mendelian inheritance in man (OMIM). *Nucleic Acids Res.*, **37**, D793–D796.
9. Hamosh,A., Scott,A.F., Amberger,J., Bocchini,C., Valle,D. and McKusick,V.A. (2002) Online mendelian inheritance in man (OMIM), a knowledgebase of human genes and genetic disorders. *Nucleic Acids Res.*, **30**, 52–55.
10. Bajdik,C.D., Kuo,B., Rusaw,S., Jones,S. and Brooks-Wilson,A. (2005) CGMIM: automated text-mining of Online Mendelian Inheritance in Man (OMIM) to identify genetically-associated cancers and candidate genes. *BMC Bioinformatics*, **6**, 78.
11. Masseroli,M., Galati,O., Manzotti,M., Gibert,K. and Pinciroli,F. (2005) Inherited disorder phenotypes: controlled annotation and statistical analysis for knowledge mining from gene lists. *BMC Bioinformatics*, **6(Suppl. 4)**, S18.
12. Hishiki,T., Ogasawara,O., Tsuruoka,Y. and Okubo,K. (2004) Indexing anatomical concepts to OMIM Clinical Synopsis using the UMLS Metathesaurus. *In Silico Biol.*, **4**, 31–54.
13. Cantor,M.N. and Lussier,Y.A. (2004) Mining OMIM for insight into complex diseases. *Medinfo*, **11**, 753–757.
14. Freudenberg,J. and Propping,P. (2002) A similarity-based method for genome-wide prediction of disease-relevant human genes. *Bioinformatics*, **18(Suppl. 2)**, S110–S115.
15. van Driel,M.A., Bruggeman,J., Vriend,G., Brunner,H.G. and Leunissen,J.A. (2006) A text-mining analysis of the human phenome. *Eur. J. Hum. Genet.*, **14**, 535–542.
16. Nelson,S.J., Schopen,M., Savage,A.G., Schulman,J.L. and Arluk,N. (2004) The MeSH translation maintenance system: structure, interface design, and implementation. *Stud. Health Technol. Inform.*, **107**, 67–69.
17. Nakazato,T., Takinaka,T., Mizuguchi,H., Matsuda,H., Bono,H. and Asogawa,M. (2008) BioCompass: a novel functional inference tool that utilizes MeSH hierarchy to analyze groups of genes. *In Silico Biol.*, **8**, 53–61.
18. Jensen,L.J., Saric,J. and Bork,P. (2006) Literature mining for the biologist: from information retrieval to biological discovery. *Nat. Rev. Genet.*, **7**, 119–129.
19. Gaudan,S., Kirsch,H. and Rebholz-Schuhmann,D. (2005) Resolving abbreviations to their senses in Medline. *Bioinformatics*, **21**, 3658–3664.
20. Horsthemke,B. and Wagstaff,J. (2008) Mechanisms of imprinting of the Prader-Willi/Angelman region. *Am. J. Med. Genet. A*, **146A**, 2041–2052.
21. Rother,K.I. (2007) Diabetes treatment—bridging the divide. *N. Engl. J. Med.*, **356**, 1499–1501.
22. McKusick,V.A. (2007) Mendelian Inheritance in Man and its online version, OMIM. *Am. J. Hum. Genet.*, **80**, 588–604.